First Confirmation that Water Ice is the Primary Component of Polar Mesospheric Clouds

Mark E. Hervig
Department of Atmospheric Science, University of Wyoming, Laramie

Robert E. Thompson, Martin McHugh, and Larry L. Gordley
G&A Technical Software Inc., Newport News, VA

James M. Russell III
Center for Atmospheric Sciences, Hampton University, VA

Michael E. Summers
School of Computational Sciences and Department of Physics and Astronomy, George Mason University, Fairfax, VA

Abstract. Polar mesospheric clouds (PMCs) have been measured in the infrared for the first time by the Halogen Occultation Experiment (HALOE). PMC extinctions retrieved from measurements at eight wavelengths show remarkable agreement with model spectra based on ice particle extinction. The infrared spectrum of ice has a unique signature, and the HALOE–model agreement thus provides the first physical confirmation that water ice is the primary component of PMCs. PMC particle effective radii were estimated from the HALOE extinctions based on a first order fit of model extinctions.

1. Introduction

Polar mesospheric clouds occur in both hemispheres near the summer solstice at high latitudes and altitudes near the mesopause (~82 km) [e.g., *Alpers et al.*, 2000]. From the ground these clouds appear in reflected sunlight against the twilight sky at solar depression angles between 7° and 16°. These sightings can be brilliant, leading ground–based observers to call them noctilucent or ”night–shining” clouds (NLCs). *Wegener* [1912] was the first to suggest that these clouds could be composed of water ice, and this theory has persisted because PMCs have been associated with ice supersaturations and because their growth appears to be an exponential function of temperature [e.g., *Rusch et al.* 1991; *Lübken et al.*, 1996]. Until now, this assertion has remained unconfirmed by observation because PMCs had only been measured at ultraviolet to near–infrared wavelengths, where unique absorption features or “fingerprints” do not exist.

Since the existence of PMCs is apparently related to temperature and water vapor, these clouds may be an excellent indicator of small changes in the global atmosphere. *Thomas et al.* [1989] suggested that the first documented appearance of PMCs in 1885 [*Backhouse*, 1885] may have been a consequence of increasing global methane (CH_4) following the start of the industrial revolution. Since CH_4 oxidizes to H_2O in the stratosphere, increased CH_4 would eventually result in increased H_2O in the upper atmosphere, and thus provide enhanced condensible vapor for PMC growth. Indeed, a recent report by *Gadsden* [1997] shows that the number of PMC sightings over northern polar regions has increased by nearly 100% during the past 35 years, and satellite observations [e.g., *Evans et al.*, 1995; *Debrestian et al.*, 1997] revealed an increase in PMC occurrence over southern high latitudes since the 1980’s [*Olivero et al.*, 1996]. Furthermore, a dramatic example occurred on June 22–23, 1999 when PMCs were observed for the first time as far south as Colorado and Utah. This unexpected low–latitude display prompted dozens of news accounts in the media. The reported increases in PMC occurrence may suggest that the upper atmosphere is becoming cooler and/or more humid over time. Cooling of the mesopause region has been suggested because of CO_2 build–up due to anthropogenic activities [*Roble and Dickenson*, 1989]. While increased CO_2 warms the lower atmosphere, it cools the upper atmosphere by direct radiative loss to space. As a result, mesospheric cloud formation has been proposed as an important manifestation of global change [*Thomas*, 1996]. It now appears that PMC occurrence is a sensitive climate indicator that has been conveying climate change information for over a century.

PMCs have been measured at eight infrared wavelengths (2.4 to 10 μm) by the Halogen Occultation Experiment (HALOE) during nine southern and nine northern polar summer seasons. A recent analysis of these measurements has isolated the PMC signals and produced particulate extinction coefficients from all eight HALOE channels. This work reports the analysis of these data, and provides comparisons with model spectra based on ice particle extinction.

Table 1. HALOE bandpass center wavelengths, bandwidth, designated absorbing species, and absorbing species at mesospheric altitudes.								
Band Center Wavelength (μm)	2.45	2.80	3.40	3.46	5.26	6.26	6.61	9.87
Bandwidth (nm)	36	53	76	50	89	43	67	773
Designated Species	HF, Aerosol	CO_2	HCl, Aerosol	CH_4, Aerosol	NO, Aerosol	NO_2	H_2O	O_3
Mesospheric Species	Aerosol	CO_2, Aerosol	Aerosol	Aerosol	NO, Aerosol	Aerosol	H_2O, Aerosol	O_3, Aerosol

2. HALOE PMC Observations

HALOE has been recording solar occultation measurements from the Upper Atmosphere Research Satellite since its activation on October 11, 1991 [*Russell et al.*, 1993]. HALOE contains eight infrared channels and produces transmission profiles for 30 occultations per day. Table 1 summarizes the HALOE bandpass characteristics and lists the designated absorbing species in addition to the important absorbers at mesospheric altitudes. HALOE provides four to six weeks of coverage at PMC latitudes near each summer solstice as shown in Figure 1. The instrument field of view (FOV) is 2 arcmin in elevation by 6 arcmin in azimuth, corresponding to about 1.5 km in altitude by 4.5 km horizontally at typical PMC tangent point altitudes. The effective vertical resolution (Δz) is increased to about 1.8 km due to optical effects and low–pass filter smoothing, and the tangent point path length (along–limb, Δx = ~305 km) is a function of the vertical resolution.

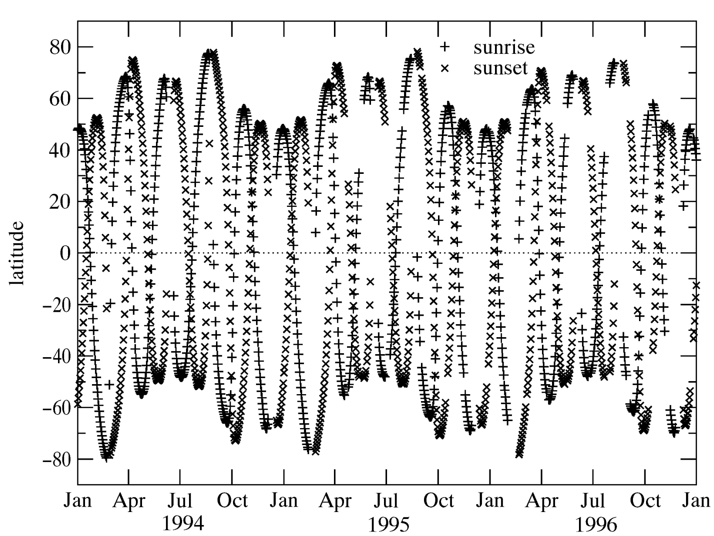

Figure 1. An example of HALOE latitude coverage for 1994 – 1996. Plotted points are daily mean latitudes for typically 15 sunrise or sunset occultations per day.

The measured signal profiles are sampled at 0.3 km vertical spacing, which is determined by the telescope scan rate and detector sampling frequency. normalized by the average observed exoatmospheric solar intensity to yield transmission, $\tau(\lambda)$, at each wavelength λ. The profiles are registered in altitude by comparing the CO_2 channel transmissions with simulations based on temperature/pressure profiles from the National Center for Environmental Protection (NCEP) at altitudes near 30 km [*Hervig et al.*, 1996]. Solar ephemeris calculations and image pointing references are used to accurately determine relative pointing and therefore tangent height for all samples. During normal production data processing, the transmission profiles are smoothed in altitude to increase the signal–to–noise ratio for the gas mixing ratio retrievals. However, this smoothing degrades thin cloud signals by smearing them over altitude. For the PMC analysis, the transmissions were reprocessed without vertical smoothing to retain sensitivity and achieve the highest possible vertical resolution (~1.8 km). Transmission is related to optical depth by $\tau(\lambda) = \exp[-\sigma(\lambda)]$, where optical depth is $\sigma(\lambda) = \beta(\lambda)\Delta x$ and $\beta(\lambda)$ is extinction coefficient. For the low values of $\sigma(\lambda)$ associated with PMCs, optical depth can be approximated by: $\sigma(\lambda) \approx 1 - \tau(\lambda)$, to much less than one percent uncertainty.

Cloud–free HALOE profiles at PMC altitudes indicate that the limb–path optical depth due to molecular absorption changes gradually over altitude. In contrast, the change in optical depth across the top edge of a PMC is relatively sharp (Figure 2). These characteristics were used to isolate the PMC signal in each HALOE channel by removing the average optical depth measured above a PMC from the average optical depth measured within a PMC. This approach assumes that the molecular absorption changes little over one FOV, and attributes the optical depth change to PMC particles. In this approach the average PMC optical depth, $\overline{\sigma}(\lambda)_i$, was estimated by:

$$3\,\overline{\sigma}(\lambda)_i = [\,\sigma(\lambda)_{i+1} + \sigma(\lambda)_i + \sigma(\lambda)_{i-1}\,] - [\,\sigma(\lambda)_{i-5} + \sigma(\lambda)_{i-6} + \sigma(\lambda)_{i-7}\,] \qquad (1)$$

where the subscript i refers to altitude (e.g., altitude i–1 is 0.3 km above altitude i). Three–point smoothing is employed to reduce noise, and changes are then characterized over the vertical resolution (1.8 km between centroids). Due to the optically thin nature of PMCs, any absorption increase is assumed to be nearly equal to the tangent path optical depth. Assuming that PMCs occupy the entire tangent path, the average extinction is therefore $\overline{\beta}(\lambda) = \overline{\sigma}(\lambda)/\Delta x$ (Δx= ~305 km for 1.8 km vertical thickness). Since PMC layers can be less than 1.8 km thick and possibly non–uniform across the 305 km path length, this approach may overestimate the actual extinctions. However, inaccuracies in path length will not affect the relative spectral signatures deduced from HALOE. This approach provides a first order removal of contaminant gaseous absorption and unknown zero–level offsets. Because the HALOE channels are temporally and spatially identical, the identical volume of air is sampled simultaneously by each channel. Therefore, by finding cloud tops and using equation 1 to estimate $\overline{\sigma}(\lambda)$ for many profiles, an average $\overline{\sigma}(\lambda)$ can be obtained with very small uncertainty in the relative extinction between channels.

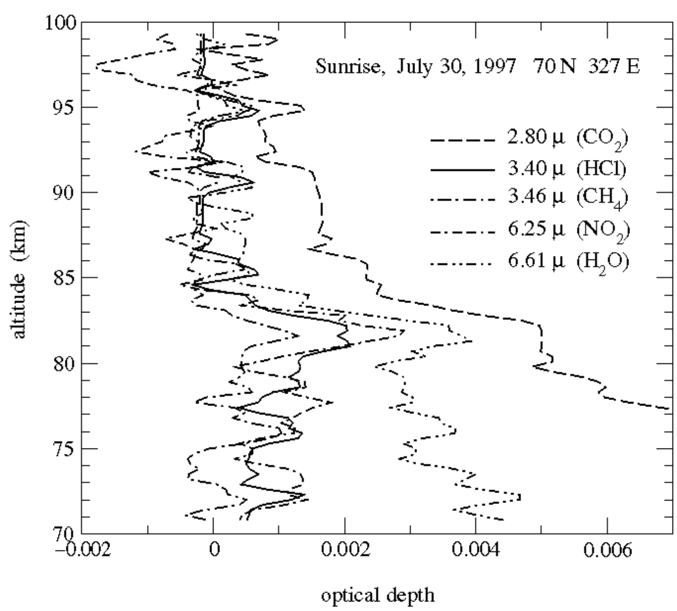

Figure 2. HALOE optical depth profiles from sunrise on July 30, 1997, at 70°N, 327°E, without the smoothing done in production data processing. A PMC signature at 81–83 km is evident as a rather sharp increase in optical depth. CO_2 absorption in the 2.80 µm channel, and H_2O absorption in the 6.61 µm channel are evident as gradual increases in optical depth. The 2.45, 5.27 and 9.87 µm channels were omitted for visual clarity.

3. Model PMC Extinction Spectra

The current understanding of PMCs suggests that these clouds are composed of ice particles. To test this assertion, PMC extinction spectra were modeled based on ice particle characteristics for comparison with the HALOE observations. The extinction cross sections of individual PMC particles were calculated using Mie theory with the complex refractive indices of ice. Extinction coefficients were then calculated by integrating the single particle cross sections over an appropriate size distribution.

Three types of ice known to exist at atmospheric pressures are ordinary hexagonal ice, cubic ice which is formed by vapor condensation at low temperatures and remains stable below about 193 K, and amorphous ice which forms by condensation at even lower temperatures and remains stable below roughly 110 to 140 K. While cubic and amorphous ice transform into hexagonal ice upon warming, hexagonal ice will maintain its form upon cooling to very low temperatures. Since PMCs form at temperatures below about 150 K, they could be composed of hexagonal, cubic, or amorphous ice. The optical properties of hexagonal and cubic ice can be considered identical [e.g., *Warren*, 1984]. The optical properties of amorphous ice are found for selected wavelengths, however, the existing data were insufficient for use in this work. This work considered refractive indices of hexagonal ice from *Bertie et al.* [1969] (measured at 100 K temperature and λ from 1.2 – 333 μm), *Warren* [1984] (266 K; 0.05 – 2000 μm), *Toon et al.* [1994] (163 K; 1.4 – 20 μm), and *Gosse et al.* [1995] (251 K; 1.4 – 7.8 μm). Gosse et al. report only the imaginary index, and recommend using the real indices from Warren. The various refractive indices are in generally good agreement at the HALOE wavelengths, with some differences near 2.5 and 10 μm (Figure 3).

The size distributions of PMC particles have been inferred from a variety of remote measurements at ultraviolet to near infrared wavelengths. *Rusch et al*. [1991] present PMC size distributions retrieved from reflectance measurements at three visible and ultraviolet wavelengths from the Solar Mesosphere Explorer (SME) satellite. Their measurement inversions assumed ice refractive indices and inferred the size distribution shape but not the total particle concentration. Their results suggest that the effective radius (R_e) of PMC particles is typically less than about 70 nm, with values occasionally near 100 nm. *von Cossart et al.* [1999] present 11 lognormal PMC size distributions derived from three–color lidar observations over Norway. Their inversions assumed ice particles, and give R_e between 38 and 86 nm. The average lognormal size distribution from their sample set is described by a median radius ($\bar{r}$) of 51 nm, distribution width (s) of 1.42, and total concentration (N) of 82 cm^{-3} (R_e = 70 nm). *Alpers et al.* [2000] present unimodal lognormal size

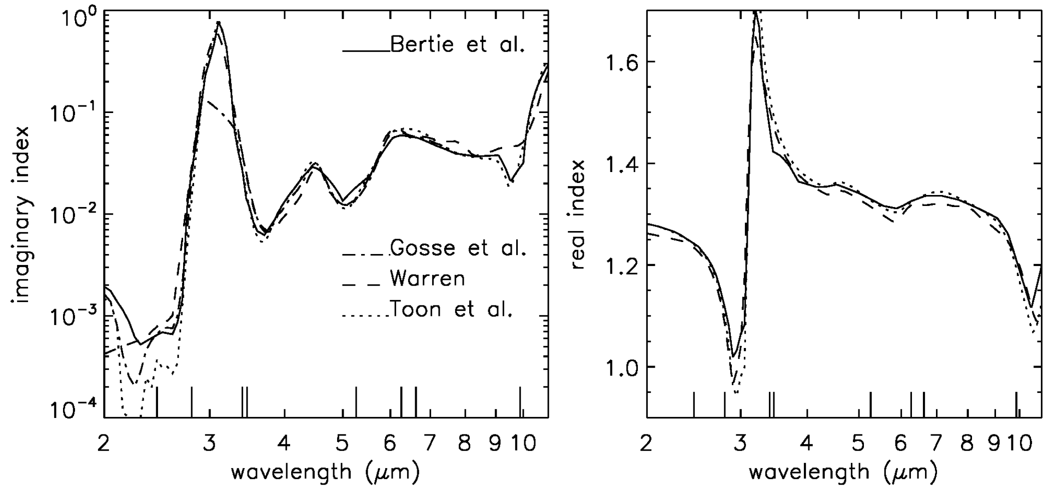

Figure 3. The imaginary refractive indices of ice from *Bertie et al*. [1969], *Warren* [1984], *Toon et al.* [1994], and *Gosse et al.* [1995]. The real refractive indices of ice from Bertie et al., Warren, and Toon et al. The locations of HALOE wavelengths are indicated by vertical lines on the abscissa.

distributions retrieved from five–color lidar observations of PMCs over Germany. Their size distributions were characterized by $\bar{r}$ = 20 – 28 nm, s = 1.5 – 1.6, and N = 260 – 610 cm^{-3} (R_e = 30 – 49 nm). In general, these clouds had higher concentrations of smaller particles compared to the results of *von Cossart et al*. [1999].

Model calculations considering the above size distributions and refractive indices were used to construct PMC extinction spectra for comparison to the HALOE measurements. Similar calculations were then used to derive relationships that can be used to infer PMC particle effective radii from the HALOE measurements. These analyses are presented below.

4. Results

Our preliminary treatment of PMC signals (equation 1) was applied to northern high latitude HALOE measurements from July 25 to August 4, 1997. PMC layers were identified using the NO_2 channel (e.g., Table 1), because this bandpass is nearly free of gaseous absorption at mesospheric altitudes and because it has one of the largest expected particle extinction cross sections. A set of 16 distinct PMC measurements was assembled by identifying the largest optical depth change in a profile at mesopause altitudes (between 78 and 90 km). These measurements were then used to infer PMC extinctions (equation 1) and to construct an average extinction for each HALOE channel.

Model PMC extinction spectra were calculated using lognormal PMC size distributions with ice refractive indices (see section 3) for comparison to the HALOE data. In the first scenario, HALOE was compared to model results based on the average PMC size distribution from *von Cossart et al.* [1999] with ice refractive indices from *Bertie et al.* [1969], *Warren* [1984], and *Toon et al.* [1994] (results using the *Gosse et al.* [1995] indices were similar to those using the Warren indices). To focus this comparison on spectral shape, each model curve was scaled to match the HALOE PMC extinction at 6.61 μm wavelength. The results show remarkable agreement between the HALOE measurements and the normalized model PMC spectra (Figure 4a). The model extinctions are similar for using the different refractive index data, except near 10 μm where the cold temperature indices result in less extinction than the warm temperature indices, and thus more closely match the HALOE measurement. Additional differences are found near 2.5 μm, with no clear separation between results based on the warm and cold temperature indices. For the second scenario, spectra were calculated using the Bertie et al. indices with 11 PMC size distributions reported by *von Cossart et al.* [1999]. This comparison evaluates the extinction magnitude as well as spectral shape by comparing unscaled model results to HALOE (Figure 4b). In this comparison, the HALOE standard deviations are generally within the range of model extinctions based on the 11 size distributions considered. The excellent agreement between HALOE and the modeled ice PMC spectra provides the first observational confirmation that the primary component of PMCs is water ice. While the current understanding of PMCs suggests that these clouds are composed of ice particles this assertion has remained a subject of debate until now. Uncertainties remained because PMC measurements were only available at ultraviolet to near–infrared wavelengths, where particulate spectra are void of unique absorption features or “fingerprints.”

PMC particle effective radii were estimated from the measured extinctions using a first order approach. By fixing the width (s) of a lognormal size distribution, a range of distributions can be generated that depend only on the effective radius, $R_e = \bar{r} \exp[\ 2.5 \ln^2(s)]$. This range of size

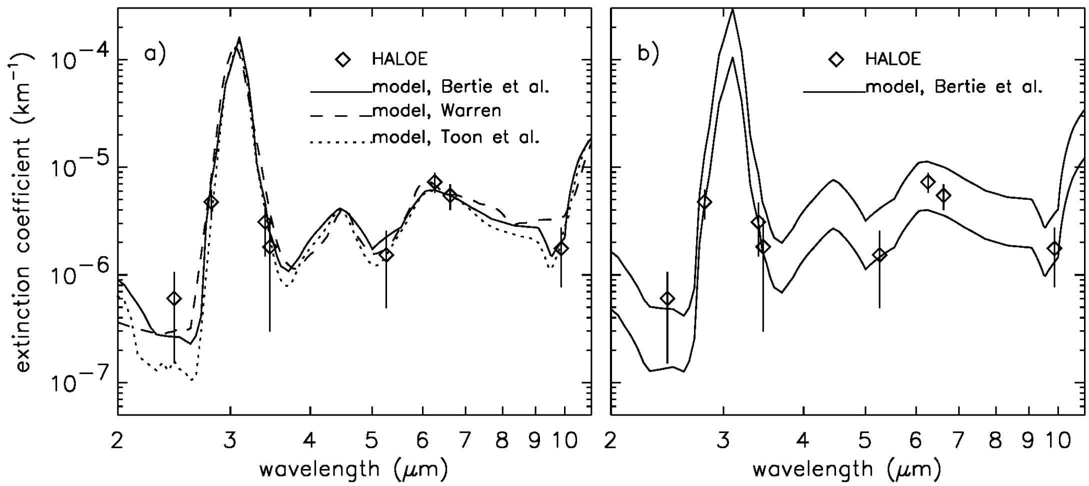

Figure 4. HALOE PMC extinctions compared to various modeled extinction spectra. The HALOE data are averages based on 16 PMC measurements from July 25 to August 4, 1997, between 62°N and 72°N latitude. Vertical bars on each HALOE point represent the standard deviation of these measurements. a) HALOE extinctions compared to model spectra calculated using the average PMC size distribution from *von Cossart et al.* [1999] with ice refractive indices from *Bertie et al.* [1969], *Warren* [1984], and *Toon et al.* [1994]. The model spectra were scaled to match the HALOE extinction at 6.61 μm wavelength. These scale factors were 0.76, 0.76, and 0.65 for results based on the Bertie et al., Warren, and Toon et al. indices. b) HALOE extinctions compared to model PMC extinction spectra calculated using the Bertie et al. refractive indices. Two model curves encompass the range of extinctions based on 11 PMC size distributions reported by von Cossart et al.

distributions was used to model relationships between R_e and the ratio of extinction at two wavelengths, independent of total particle concentration. These results indicate that HALOE extinction ratios based on the HF channel, $\beta(\lambda)/\beta(2.45)$, are uniquely dependent on effective radius for R_e > ~20 nm (Figure 5). As a result, the measured ratios can be used to determine R_e by interpolating from modeled curves. The HALOE PMC extinctions from Figure 4 were used with model relationships based on the Bertie et al. refractive indices to estimate R_e for the seven HALOE extinction ratios (Figure 5). These results give $R_e = 94 \pm 14$ nm (average ± standard deviation) for s = 1.8. Using s = 1.5 gives $R_e = 128 \pm 18$ nm and using s = 2.1 gives $R_e = 69 \pm 11$ nm. The standard deviation of the effective radii estimates from seven ratios is only 15%, indicating that the HALOE PMC measurements are internally consistent. The effective radii determined from HALOE are slightly larger than indicated by previous studies. This may be a result of selecting only PMCs with very strong signatures for this study, so chosen to more accurately characterize their spectrum. These clouds may have been more mature than average, and thus characterized by larger particles sizes according to simple condensational growth theory. Another factor is that the typical response to a PMC by the 2.45 μm channel is expected to be very low (Figure 4). As a result, the average 2.45 μm extinction from the 16 PMC sample could be biased toward high PMC extinctions, which would in turn bias the estimates of R_e toward larger sizes. Nevertheless, previous results [e.g., *von Cossart et al.*, 1999] were based on visible measurements, and it is possible that the infrared measurements from HALOE will shed new light on the properties of PMCs. Results using the other ice refractive indices are similar to those above using the *Bertie et al.* [1984] indices. While the initial estimates of R_e leave room for improvement, they suggest potential for the HALOE observations to reliably characterize PMC size distribution moments, and possibly size distributions. Reduced uncertainty in future HALOE PMC extinction retrievals combined with more rigorous inversions will improve and expand upon the analysis presented here.

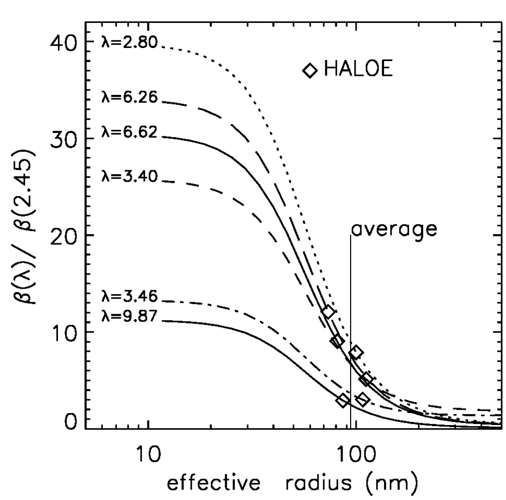

Figure 5. Effective radius (R_e) versus extinction ratio from model calculations (curves) based on ice refractive indices from *Bertie et al.* [1969] and lognormal size distributions with fixed width (s = 1.8). Measured PMC extinction ratios based on the HALOE data in Figure 4 were overplotted on the model curves to give estimates of R_e, and the average R_e (94 nm) is indicated. Results for the 5.26 μm channel were eliminated for visual clarity.

5. Conclusions

This report offers the first measurements of the infrared signature of PMCs between 2.45 μm and 10 μm wavelength. PMC extinctions derived from eight HALOE channels show remarkable agreement with model PMC spectra based on ice particle extinction, and thus provide the first observational confirmation that water ice is the primary component of PMCs. A first order fit to the HALOE PMC extinctions suggests the cloud particle effective radius was between 69 and 128 nm. The preliminary analyses offered here suggest the great potential for HALOE measurements to advance the knowledge of PMCs, and future efforts will more rigorously assess these observations.

Acknowledgements. This paper combines efforts funded under under three NASA grants: NAS5–98076 and NAG–7001 under the NASA MTPE program and NAG5–9669 under the NASA ITM program. The authors thank Ellis Remsberg, Lance Deaver, and Anju Shah for many helpful discussions, continued HALOE operation, and production of HALOE data.

References

Alpers, M., M. Gerding, J. Hoffner, and U. von Zahn, NLC particle properties from a five color lidar observation at 54°N, *J. Geophys. Res., 105,* 12,235–12,240, 2000.

Backhouse, T. W., The luminous cirrus cloud of June and July, *Meteorol. Mag*., *20,* 33, 1885.

Bertie, J. E., H. J. Labbe, and E. Whalley, Absorptivity of ice I in the Range 4000–30 cm^{-1}, *J. Chem. Phys*., *50,* 4501–4520, 1969.

Debrestian, D. J., J. D. Lumpe, E. P. Shettle, R. M. Bevilacqua, J. J. Olivero, J. S. Hornstein, W. Glaccum, D. W. Rusch, C. E. Randall, and M. D. Fromm, An analysis of POAM II solar occultation observations of polar mesospheric clouds in the southern hemisphere, *J. Geophys. Res*., *102,* 1971–1981, 1997.

Evans, W. F. J. , L. R. Laframboise, K. R. Sine, R. H. Wiens and G. G. Shepherd, Observation of polar mesospheric clouds in summer, 1993 by the WINDII instrument on UARS, *Geophys. Res. Lett.*, *22*, 2793–2796, 1995.

Gadsden, M. The secular change in noctilucent cloud occurrence: Study of a 31–year sequence to clarify the causes, Adv. Space Res., 20, 2097–2100, 1997.

Gosse, S., D. Labrie, and P. Chylek, Petr, Refractive index of ice in the 1.4–7.8–μm spectral range, *Applied optics*, v 34 n 28, p6582, 1995.

Hervig M. E., J. M. Russell III, L. L. Gordley, S. R. Drayson, K. Stone, R. E. Thompson, M. E. Gelman, I. S. McDermid, A. Hauchecorne, P. Keckhut, T. J. McGee, U. N. Singh, and M. R. Gross, Validation of temperature measurements from the Halogen Occultation Experiment, *J. Geophys. Res., 101*, 10,277–10,285, 1996.

Lübken, F–J., K. H. Fricke, and M. Langer, Noctilucent clouds and the thermal structure near the Arctic mesopause in summer, *J. Geophys. Res., 101*, 9489–9508, 1996.

Olivero, J. J., and G. E. Thomas, Climatology of polar mesospheric clouds, *J. Atmos. Sci., 43*, 1263–1274, 1986.

Olivero, J.J., G. E. Thomas, W. Evans, D. Debrestian and E. Shettle, Three satellite comparison of polar mesospheric cloud properties: A first look, *Trans. American Geophys. Union, 77*, F119, 1996.

Roble, R. G., and R. E. Dickenson, How will changes in carbon dioxide and methane modify the mean structure of the mesosphere and thermosphere?, *Geophys. Res. Lett., 16,* 1441–1444, 1989.

Rusch, D. W., G. E. Thomas, and E. J. Jensen, Particle size distributions in polar mesospheric clouds derived from solar mesosphere explorer measurements, *J. Geophys. Res., 96*, 12,933–12,939, 1991.

Russell, J. M. III, L. L. Gordley, J. H. Park, S. R. Drayson, W. D. Hesketh, R. J. Cicerone, A. F. Tuck, J. E. Frederick, J. E. Harries, and P. J. Crutzen, The Halogen Occultation Experiment, *J. Geophys. Res*., *98*, 10,777–10,797, 1993.

Thomas, G. E., Is the polar mesosphere the miner's canary of global change?. *Adv. Space Res.*, *18*, 149–158, 1996.

Thomas, G.E. and J.J. Olivero, Climatology of Polar Mesospheric Clouds. 2. Further analysis of Solar Mesosphere Explorer Data, *J. Geophys. Res., 94*, 14,673–14,681, 1989.

Toon O. B., M. A. Tolbert, B. G. Koehler, A. M. Middlebrook, and J. Jordan, Infrared optical constants of H_2O ice, amorphous nitric acid solutions, and nitric acid hydrates, *J. Geophys. Res.*, *99*, 25,631–25,645, 1994.

Warren, S. G., Optical constants of ice from the ultraviolet to the microwave, *Appl. Optics*, *23*, 11.906–11.926, 1984.

von Cossart, G., J. Fiedler, and U. von Zahn, Size distributions of NLC particles as determined from 3–color observations of NLC by ground–based lidar, *Geophys. Res. Lett.*, *26*, 1513–1516, 1999.

Wegener, A., Die Erforschung der obersten Atmospharenschichten, *Gerlands Beitr. Geophys.*, *11*, 102, 1912.